Z. Phys. A – Atoms and Nuclei 316, 161–167 (1984)

Zeitschrift für Physik A Atoms and Nuclei

On the Effect of Off-Shell Wavefunctions on K and L Shell Charge Transfer in Fast, Asymmetric Collisions

D.H. Jakubaßa-Amundsen

Physik-Department, Technische Universität München, Garching, Federal Republic of Germany

Received October 18, 1983

Within the semiclassical strong potential Born approximation (SPB) we have calculated the electron capture from the K and L shell of a heavy target atom by protons using two different peaking approximations. Both total capture cross sections and impact parameter distributions are compared with the impulse approximation (IA) and in the case of transfer from the Ar K-shell also with an exact evaluation of the SPB and with experimental data. While for the K shell, all theories give a similar impact-parameter dependence, there is a substantial difference between IA and SPB results for the $2s$ subshell.

1. Introduction

The theory of charge exchange in fast ion-atom collisions has received much interest lately. For asymmetric collision systems, the strong potential Born approximation, which is a consistent first-order theory with respect to the weaker of the two atomic potentials, has become established as an appropriate theory for projectile velocities v which are much greater than the electron velocity in the bound state of the lighter nucleus [1].

The difference between the SPB and the earlier theory for charge exchange, the impulse approximation [2, 3], lies in the fact that the intermediate state, into which the electron is excited, being an off-shell state in the exact formulation, is replaced in the IA by its on-shell value, a continuum Coulomb wave. Although the difference between the off-shell and on-shell energy is of the order of the weak field (in our case the projectile with charge Z_P), the error introduced into the IA depends strongly on the potential of the heavier collision partner (the target with charge Z_T), due to the nonuniform convergence of an off-shell state to an on-shell one [4, 5].

In the case of transfer from the target K shell, it has been found that at large collision velocities which exceed the electron orbiting velocity v_e of the target bound state, the two theories may deviate from each other by 50% or even more [5, 6]. However, no test of the SPB theory exists for capture from the L shell. The only data which include L-shell capture [7] can not be explained by the IA, indeed, for the collision system (p, Ar) which should be asymmetric enough for the SPB and related theories to work, the theoretical results underestimate the data by a factor of 4 at high v [8]. It is the aim of this paper to show whether an SPB calculation will improve the agreement between theory and experiment.

At intermediate velocities, $v \lesssim v_e$, the deviation of the SPB from the impulse approximation is considerably larger than for higher v [4–6]. Although the inclusion of the off-shell effect in the SPB gives more than just a correction term of the order of Z_P/Z_T, the question arises whether other higher-order contributions in the expansion of the Green's function in terms of Z_P/Z_T might also be important, thus indicating the limitation of the SPB theory.

Up to now, any calculations within the strong potential Born approximation have been carried out with the help of a peaking approximation, either the Briggs' peaking [3] where the intermediate momentum of the electron is replaced by $\mathbf{v}$, which means that terms of the order of $(Z_P/v)^2$ are consistently neglected [4, 6, 9], or a less restrictive peaking, also called "transverse peaking" where in the excitation matrix element only the momentum components perpendicular to $\mathbf{v}$ are neglected, while the third component is fixed by energy conservation [5, 10].

Thereby the difference to IA results depends on the choice of the peaking approximation applied, and although Briggs' peaking should be better for SPB than for IA [10], the question of validity of the SPB can only be decided by means of an exact evaluation of the strong potential Born theory.

Apart from the comparison with the impulse approximation it is necessary to find out to which extent the exact SPB can reproduce the experimental data, as it does not seem possible to evaluate without peaking any theory which goes beyond SPB. For the capture from the Ar K-shell by protons, early experiments [11] have been carefully redone by two independent groups [12], but there remains a discrepancy with the peaked SPB at intermediate velocities.

In this paper the exact SPB is evaluated for the case of $1s-1s$ transitions, using the representation of the off-shell excitation matrix element given by Macek and coworkers [13, 6] (Sect. 2.1). For the transfer from the L subshells, the transverse peaking is applied, and in the case of a $2s$ initial state, a new approximation is introduced where apart from the replacement of the off-shell state by a renormalised Coulomb wave, no further peaking approximation is made (Sect. 2.2). In Sect. 3, the numerical methods are described, and Sect. 4 gives a comparison between SPB and IA both with and without peaking approximations, as well as with experimental data for the (p, Ar) collision system. Thereby total cross sections and also impact parameter distributions are investigated. A short conclusion follows (Sect. 5). Atomic units ($\hbar=m=e=1$) are used unless otherwise indicated.

2. Theory

In the semiclassical approximation, the amplitude for the transfer of a target electron, described by ψ_i^T to a final projectile state, ψ_f^P, can be written as

$$a_{fi}=-i\int_{-\infty}^{\infty} dt\langle\psi_f^{(-)}(t)|\,V_P(\mathbf{r}-\mathbf{R})|\psi_i^T(t)\rangle \tag{2.1}$$

where V_P is the projectile field and the internuclear trajectory $\mathbf{R}(t)$ is described by a straight-line path with impact parameter $\mathbf{b}$. The state $\psi_f^{(-)}$ is an exact solution of the three-body scattering problem which obeys the correct asymptotic boundary conditions.

In the strong potential Born approximation, terms proportional to the weak field V_P are neglected in the expansion of the scattering state, however, V_P enters through the boundary condition which has the effect of shifting the wavefunction off the energy shell. With this approximation, the transition amplitude is given by [14]

$$a_{fi}=-i\int_{-\infty}^{\infty} dt\int d\mathbf{k}\, e^{i(E_f(\mathbf{k})-E_i^T)t}e^{i\mathbf{kb}}\varphi_f^{*P}(\mathbf{k}-\mathbf{v})\cdot\langle\psi_{\mathbf{k},E_f}|V_P|\psi_i^T\rangle,\quad E_f(\mathbf{k})=E_f^P+\mathbf{kv}-v^2/2 \tag{2.2}$$

where φ_f^P is the Fourier transformed final projectile state and E_i^T and E_f^P the electron energies in the initial and final state, respectively. The off-shell wavefunction $\psi_{\mathbf{k},E_f}$ is defined by means of

$$(E_f-i\varepsilon-H_T)|\psi_{\mathbf{k},E_f}\rangle=(E_f-k^2/2-i\varepsilon)|\mathbf{k}\rangle$$
$$H_T=T+V_T \tag{2.3}$$

where T is the kinetic energy, V_T the target field and $|\mathbf{k}\rangle$ a plane wave.

2.1. Exact Evaluation of the SPB Amplitude

If the off-shell function is decomposed according to

$$|\psi_{\mathbf{k},E_f}\rangle=|\mathbf{k}\rangle+|\chi_{\mathbf{k},E_f}\rangle \tag{2.4}$$

and the Fourier representation of the projectile field is introduced, the matrix element $M_2=\langle\chi_{\mathbf{k},E_f}|\exp(i\mathbf{sr})|\psi_i^T\rangle$ which is needed for the evaluation of (2.2) has been given for a $1s$ initial state in terms of a single integral [13] and shown to reduce further to an analytical expression [6]

$$M_2=-\frac{2^{3/2}iZ_T^{7/2}}{\pi D_1\eta}\frac{d}{d\mu}\left\{\frac{1}{F\sqrt{B^2-C}}\left[\frac{1}{(1-i\eta)\rho_+}\cdot{}_2F_1\left(1,1-i\eta,2-i\eta,\frac{1}{\rho_+}\right)-\frac{i\pi}{\sinh\pi\eta}(-\rho_-)^{-i\eta}-\frac{1}{i\eta}\,{}_2F_1(1,i\eta,1+i\eta,\rho_-)\right]\right\}\Bigg|_{\mu=Z_T} \tag{2.5}$$

$$\eta=Z_T/K,\quad K=\sqrt{2E_f(\mathbf{k})+i\varepsilon}$$

$$\rho_\pm=B\pm\sqrt{B^2-C},\quad B=\frac{-4\mathbf{ks}K^2+E_1E_2}{D_1F},$$
$$C=D_2/F$$
$$D_1=-K^2+k^2,\quad E_1=-K^2-k^2$$
$$D_2=(\mu-iK)^2+s^2,\quad E_2=-K^2-\mu^2-s^2$$
$$F=(\mu+iK)^2+s^2.$$

Thereby the initial state has been parametrised as $\psi_i^T=(Z_T^{3/2}/\sqrt{\pi})\exp(-\mu r)$ and ${}_2F_1$ is a hypergeometric function. In the derivation of (2.5) use has been made of the peaking condition $|\mathbf{k}-\mathbf{v}|\lesssim Z_P$ and $Z_P/v\ll 1$ in order to determine the pole positions ρ_+

and ρ_- of the integrand. However, the result (2.5) is independent of whether ρ_+ or ρ_- lie inside or outside the unit circle as the hypergeometric functions can be continued analytically when the poles cross $|\rho|=1$ and give the same result as would be obtained from a direct integration. From this it follows that (2.5) is exact.

Carrying out the differentiation with respect to μ and using the Gauss relations for the hypergeometric functions [15], M_2 can be written in terms of two ${}_2F_1$-functions:

$$M_2 = -\frac{2^{3/2} i Z_T^{7/2}}{\pi \eta F} M_{20} \tag{2.6}$$

$$\begin{aligned} M_{20} = \frac{1}{D_1 \sqrt{B^2 - C}} \Bigg\{ & {}_2F_1\left(1, 1-i\eta, 2-i\eta, \frac{1}{\rho_+}\right) \\ & \cdot \frac{1}{(1-i\eta)\rho_+}\left[-\frac{F'}{F} - \frac{2BB'-C'}{2(B^2-C)} - \frac{i\eta}{\rho_+}\rho'_+\right] \\ & - \left[{}_2F_1(1, i\eta, 1+i\eta, \rho_-)\frac{1}{i\eta} + \frac{i\pi}{\sinh \pi\eta}(-\rho_-)^{-i\eta}\right] \\ & \cdot \left[-\frac{F'}{F} - \frac{2BB'-C'}{2(B^2-C)} - \frac{i\eta}{\rho_-}\rho'_-\right] \\ & - \frac{1}{\rho_+(\rho_+-1)}\rho'_+ - \frac{1}{\rho_-(1-\rho_-)}\rho'_- \Bigg\} \end{aligned}$$

where a prime indicates the derivative with respect to μ which is set equal to Z_T afterwards.

An extension to higher initial states ψ_i^T is straightforward, as the corresponding matrix elements can be expressed by means of partial derivatives of (2.6) with respect to μ and $\mathbf{s}$, in the same way as done in the case of the impulse approximation [8].

The additional term in the excitation matrix element, $\langle \mathbf{k} | \exp(i\mathbf{s}\mathbf{r}) | \psi_i^T \rangle$, which arises from the plane wave in (2.4), is just the Fourier transform $\varphi_i^T(\mathbf{k}-\mathbf{s})$ of the initial state.

For the subsequent evaluation of the transition amplitude, it is convenient to replace the variable $\mathbf{k}$ by $\mathbf{q}_0 = \mathbf{k} - \mathbf{s}$ and to introduce spherical coordinates. Then the capture amplitude follows from

$$\begin{aligned} a_{fi} = \frac{iZ_P}{\pi} \int d\mathbf{q}_0 e^{i\mathbf{q}_0\mathbf{b}} \delta(\Delta E - v^2/2 + \mathbf{q}_0\mathbf{v}) \\ \cdot \int \frac{d\mathbf{s}}{s^2} \varphi_f^{*P}(\mathbf{q}_0 + \mathbf{s} - \mathbf{v}) [\varphi_i^T(\mathbf{q}_0) + M_2(\mathbf{q}_0, \mathbf{s})] \end{aligned} \tag{2.7}$$

with $\Delta E = E_f^P - E_i^T$. If the angular variables $\cos\vartheta_{\mathbf{q}_0,\mathbf{v}}$ and $x = \cos\vartheta_{\mathbf{s},\mathbf{v}}$ are introduced, the integration over the direction $\hat{\mathbf{q}}_0$ is easily performed, leading to a Bessel function J_0, while the three-dimensional integral over $\mathbf{s}$ has to be done numerically. However, the quantity K (and thus η, D_2, E_2 and F) is then independent of the azimuthal angle φ_s such that the pole structure of M_2 is irrelevant for the innermost integration. The transition amplitude for an initial and final $1s$ state is finally obtained by

$$\begin{aligned} a_{fi} = \frac{16i(Z_P Z_T)^{5/2}}{v} \int_{q_{\min}}^{\infty} q_0 dq_0 J_0(q_0 b \sin\vartheta_{\mathbf{q}_0,\mathbf{v}}) \\ \cdot \left[\frac{1}{(Z_T^2+q_0^2)^2} \frac{1}{Z_P^2+q_0^2+2\Delta E} - \frac{2iZ_P Z_T}{\pi^2} \int_0^\infty ds \right. \\ \left. \cdot \int_{-1}^{1} dx \frac{1}{\eta F} \int_0^\pi d\varphi_s \frac{1}{D_1^2} M_{20}(q_0, s, x, \varphi_s)\right] \end{aligned} \tag{2.8}$$

where $\cos\vartheta_{\mathbf{q}_0,\mathbf{v}} = (-\Delta E/v + v/2)/q_0$ and $q_{\min} = q_0 |\cos\vartheta_{\mathbf{q}_0,\mathbf{v}}|$, and we have used that $D_1 = Z_P^2 + (\mathbf{q}_0 + \mathbf{s} - \mathbf{v})^2$ which follows from $E_f^P = -Z_P^2/2$.

2.2. Peaking Approximations

The evaluation of the transition amplitude is greatly simplified if instead of the exact off-shell function, defined by (2.3), its limit for $E_f \to k^2/2$ is taken:

$$\begin{aligned} \psi_{\mathbf{k},E_f} \approx \left(\frac{2E_f - i\varepsilon - k^2}{4(2E_f - i\varepsilon)}\right)^{i\eta_0} \Gamma(1 - i\eta_0) \\ \cdot e^{-\pi\eta_0/2} \psi_{\mathbf{k}}^T, \quad \eta_0 = Z_T/k, \ \varepsilon \to 0 \end{aligned} \tag{2.9}$$

which means that $\psi_{\mathbf{k},E_f}$ is approximated by a renormalised target Coulomb wave. This approximation, which we will call the "renormalised peaking approximation" (RP), is accurate up to terms of the order of V_P and has been shown [4] to be consistent with Briggs' peaking. It is justified for large momentum transfer because in this case the excitation matrix element will mainly depend on the small-r part of $\psi_{\mathbf{k},E_f}$ for which (2.9) is a reasonable approximation [5], however, it may break down at intermediate collision velocities when the momentum transfer is low.

All peaking approximations are based on the fact that the integrand which appears in the formula (2.2) for the transition amplitude, is strongly peaked at $\mathbf{k} = \mathbf{v}$ where the Fourier transform $\varphi_f^P(\mathbf{k}-\mathbf{v})$ has its maximum. While Briggs' peaking consists in replacing $\mathbf{k}$ by $\mathbf{v}$ everywhere except in the prefactor $(2E_f - i\varepsilon - k^2)^{i\eta_0}$ in (2.9), such that the result of the $\mathbf{k}$-integration is simply proportional to the final state wavefunction at $\mathbf{r} = 0$, the transverse peaking only neglects those components of $\mathbf{k}$ in the Coulomb wave $\psi_{\mathbf{k}}^T$ of (2.9) which are perpendicular to $\mathbf{v}$, while k_z, the component of $\mathbf{k}$ parallel to $\mathbf{v}$, is determined from energy conservation. This extends the range of validity to smaller collision velocities [14, 10], and also introduces a dependence on the asymmetry, Z_P/Z_T, into the off-shell normalisation factor.

When the substitution $\mathbf{q}=\mathbf{k}-\mathbf{v}$ is made in (2.2), and (2.9) is inserted for the off-shell function, the transverse peaking approximation leads to

$$a_{fi}^{\mathrm{TP}}=\frac{iZ_P}{2\pi^2}\int_{-\infty}^{\infty} dt \int \frac{d\mathbf{s}}{s^2}\, e^{i(\Delta E+v^2/2-\mathbf{s}\mathbf{v})t}\, e^{-i\mathbf{s}\mathbf{b}}$$
$$\cdot\,\Gamma(1+i\bar{\eta})e^{-\pi\bar{\eta}/2}[4(2E_f^P+2q_z v+v^2+i\varepsilon)]^{i\bar{\eta}}$$
$$\cdot\,\langle \psi^T_{q_z\mathbf{e}_z+\mathbf{v}}|e^{i\mathbf{s}\mathbf{r}}|\psi_i^T\rangle\, I(R) \qquad (2.10)$$
$$I(R)=\int d\mathbf{q}\, e^{i\mathbf{q}\mathbf{R}}(2E_f^P-q^2+i\varepsilon)^{-i\bar{\eta}}\varphi_f^{*P}(\mathbf{q})$$
$$=4\pi^{1/2}e^{\pi\bar{\eta}}Z_P^2\frac{(2Z_P)^{-i\bar{\eta}}}{\Gamma(2+i\bar{\eta})}R^{1/2+i\bar{\eta}}K_{1/2+i\bar{\eta}}(Z_P R)$$

for a final $1s$ state, where $\bar{\eta}=Z_T/|q_z+v|$, $q_z=-\Delta E/v-v/2+s_z$ and K_ν is a modified Bessel function. Thereby it is, as in the case of Briggs' peaking, important not to make the peaking approximation in the term $2E_f^P-q^2+i\varepsilon=-(Z_P^2+q^2)+i\varepsilon$ because it has the same q-dependence as $\varphi_f^P(\mathbf{q})$. The time integral can also be carried out analytically for a straight-line trajectory [5], and with $x=\cos\vartheta_{\mathbf{s},\mathbf{v}}$ the transition amplitude for an arbitrary initial state is

$$a_{fi}^{\mathrm{TP}}=\frac{2^{3/2}i}{\pi v}Z_P^{7/2}\int_0^{\infty} ds\int_{-1}^{1} dx[4(E_i^T+svx+i\varepsilon)]^{i\bar{\eta}}$$
$$\cdot\,\frac{e^{\pi\bar{\eta}/2}b^{1+i\bar{\eta}}}{1+i\bar{\eta}}\,\frac{K_{1+i\bar{\eta}}(b\sqrt{Z_P^2+q_z^2})}{(Z_P^2+q_z^2)^{1/2+i\bar{\eta}/2}}F_i(s,x) \qquad (2.11)$$

$$F_i(s,x)=\int_0^{2\pi} d\varphi_s e^{-i\mathbf{s}\mathbf{b}}\langle\psi^T_{q_z\mathbf{e}_z+\mathbf{v}}|e^{i\mathbf{s}\mathbf{r}}|\psi_i^T\rangle$$

For capture from the L shell, it is only the $m=1$ state for which the ionisation matrix element depends on the azimuthal angle φ_s. Using the closed expression for the matrix elements [2, 8], F_i is readily obtained as

$$F_{2s}(s,x)=F_0J_0(sb\sqrt{1-x^2})$$
$$\cdot\left\{(1+i\bar{\eta})\left[\frac{2A}{B}+\frac{i}{2}Z_T|q_z+v|(2+i\bar{\eta})^2\frac{A}{B^2}\right]\right.$$
$$\left.+(1-i\bar{\eta})\left[2-Z_T^2(2+i\bar{\eta})\frac{1}{B}-\frac{1}{2}Z_T^2(2-i\bar{\eta})\frac{1}{A}\right]\right\}$$

$$F_{2p,m=0}(s,x)=-\frac{iZ_TF_0}{B}J_0(sb\sqrt{1-x^2})$$
$$\cdot\left\{(q_z+v-s_z)(1-i\bar{\eta})\left[2+i\bar{\eta}+(2-i\bar{\eta})\frac{B}{A}\right]\right.$$
$$\left.-s_z\left[i\bar{\eta}(1-i\bar{\eta})+(1+i\bar{\eta})(2+i\bar{\eta})\frac{A}{B}\right]\right\}$$

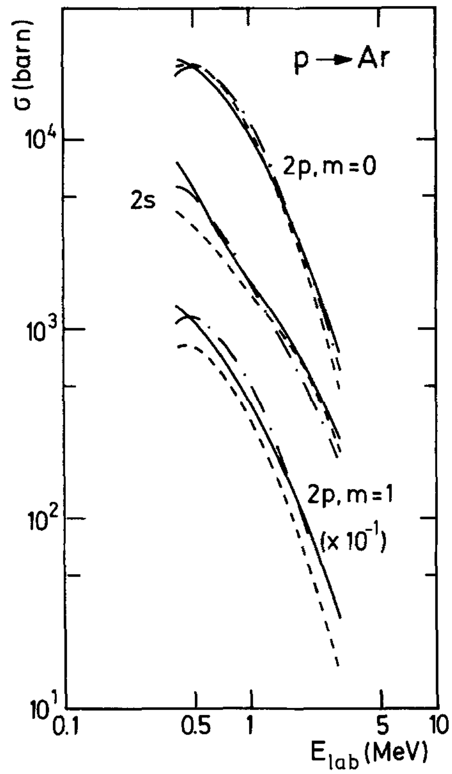

Fig. 1. Cross section for charge transfer from the L subshells of Ar into the ground state of H as a function of projectile energy. Full curves are transverse peaked SPB calculations, chain curves are IA and broken curves are transverse peaked IA calculations

$$F_{2p,m=1}(s,x)=\frac{Z_TF_0}{2^{1/2}B}J_1(sb\sqrt{1-x^2})s\sqrt{1-x^2}$$
$$\cdot\left\{2(1+\bar{\eta}^2)+(1-i\bar{\eta})(2-i\bar{\eta})\frac{B}{A}+(1+i\bar{\eta})(2+i\bar{\eta})\frac{A}{B}\right\} \qquad (2.12)$$
$$F_0=Z_T^{5/2}e^{\pi\bar{\eta}/2}\Gamma(1-i\bar{\eta})\frac{B^{-i\bar{\eta}}}{A^{2-i\bar{\eta}}},$$
$$A=Z_T^2/4+(q_z\mathbf{e}_z+\mathbf{v}-\mathbf{s})^2,$$
$$B=s^2-(|q_z+v|+iZ_T/2)^2.$$

Thus the calculation of the capture amplitude requires only a double integration. Thereby we found it convenient to express the function K_ν in terms of a hypergeometric function [15] except for large arguments (>5) where $K_\nu(x)\approx(\pi/2x)^{1/2}\exp(-x)$ is used.

In the case of the impulse approximation, where the renormalisation factor in the intermediate wavefunction (2.9) is dropped, there is a rather large difference in the capture cross section, depending on whether the transverse peaking is applied or not, especially for the $2s$ and $2p, m=1$ initial state (cf. Fig. 1). Therefore we study the transfer amplitude by using the approximation (2.9) for the off-shell wavefunction, but without any further simplification, which corresponds to the exact IA modified by the off-shell normalisation factor. Then an expression similar to (2.7) is obtained for the transfer amplitude, and one has for initial s states (and a final $1s$ state)

$$a_{fi}^{\mathrm{RP}} = \frac{2^{5/2} i Z_P^{7/2}}{\pi v} \int_{q_{\min}}^{\infty} q_0 \, dq_0 \, J_0(q_0 b \sin \vartheta_{\mathbf{q}_0,\mathbf{v}}) \int_0^{\infty} ds \int_{-1}^{1} dx \cdot e^{\pi\eta_0/2} \Gamma(1+i\eta_0) 4^{i\eta_0} \langle \psi_{\mathbf{q}_0+\mathbf{s}}^T | e^{i\mathbf{s}\mathbf{r}} | \psi_i^T \rangle \cdot \int_0^{2\pi} d\varphi_s \frac{(-Z_P^2 + i\varepsilon + 2\mathbf{v}(\mathbf{q}_0+\mathbf{s}) - v^2)^{i\eta_0}}{[Z_P^2 + (\mathbf{q}_0+\mathbf{s}-\mathbf{v})^2]^{2+i\eta_0}} \tag{2.13}$$

with $\eta_0 = Z_T/|\mathbf{q}_0+\mathbf{s}|$ and $q_{\min}$ as defined earlier. Contrary to the IA, the integral over φ_s is no longer trivial (leading to a generalised hypergeometric function F_1) such that we preferred to do all four integrals numerically.

3. Numerical Methods

While the evaluation of the transverse peaked SPB amplitude is fast and unproblematic, the calculation of charge transfer within the exact SPB theory needs special consideration. The essential difference between the integrand of (2.8) and the peaking versions (2.11)–(2.13) is that the latter has only a branch cut at $\eta \to \infty$ while the exact SPB matrix element contains an infinite number of first-order poles at $i\eta = n$ ($n = 1, 2 \ldots$) which accumulate at $\eta \to \infty$. They correspond to the bound states in the off-shell wavefunction which are neglected in the renormalised Coulomb wave (2.9). We found that the contribution of these poles is rather important for low momentum transfer ($q_0 \approx q_{\min}$), but it is completely dominated by the contribution to the integrand from the peaking value $\mathbf{s} = \mathbf{v} - \mathbf{q}_0$ at high momenta $q_0/q_{\min} \gg 1$.

In terms of the variables introduced in (2.8), the singularities appear in the x-integration at $x_n = (Z_P^2 + 2\Delta E - Z_T^2/n^2)/(2sv)$, and it depends on the value of s, how many of them lie in the interval $[-1, +1]$. These first-order poles lead to logarithmic singularities in the subsequent s-integration at $s_n = |Z_P^2 + 2\Delta E - Z_T^2/n^2|/(2v)$. We found it sufficient to include about five poles, because their importance decreases with n. For those values of s, where the accumulation point lies below $x = 1$, we used the trapezoidal integration rule from the midpoint between the 5^{th} and the 6^{th} pole to x slightly above the accumulation point. For the evaluation of the x-integration, we splitted the interval $[-1, 1]$ at the poles, zero and their midpoints and used a logarithmic variable transformation $y = \ln[\pm(x_i - x)]$ for $x \lessgtr x_i$ in the neighbourhood of the i^{th} pole. The s-integration has to be splitted accordingly, but a variable transformation is not necessary. For a fixed value of q_0, the maximum of the s-integrand at $\mathbf{s} = \mathbf{v} - \mathbf{q}_0$ (apart from the logarithmic divergences) is always (for $Z_P/v < 1$) at an s value which is higher than the accumulation point $s_\infty = (Z_P^2 + 2\Delta E)/(2v)$, such that there is no interference between the peaking point and the singularities. However, as the integrand is then strongly peaked around $\varphi_s \approx \pi$ ($\mathbf{s}$ and $\mathbf{q}_0$ lie in opposite half-planes), we found it necessary to use also a logarithmic variable for the φ_s-integration in the region of the maximum of the s-integrand.

Although not many points are needed for every x and s interval ($\sim$20–30), the computer time is tremendous. After the three innermost integrations are done, the q_0-integrand is a smooth function such that we could use an interpolation routine when doing the last integral. Note that the impact parameter enters only through the Bessel function J_0 and thus appears only in the last integration.

4. Comparison between the Theories and with Experiment

We have calculated the capture probabilities from the target K and L shell for protons colliding with Ar. Only capture to the ground state is considered. Hydrogenic wavefunctions (with Slater screening for the L-shell) and experimental binding energies were used. We estimate the accuracy of our calculations to be about 1% for the transverse peaked and for the exact SPB, and somewhat lower (5–10%) for the RP approximation at the smallest velocities.

Figure 1 shows the capture probabilities from the $2s$, $2p, m=0$ and $2p, m=1$ subshells (multiplied by the number of states with $|m| = 0$ or 1). Results are given for the (exact) IA, as well as for the transverse peaked IA and SPB theories. For the dominating contribution to the total L-shell capture, i.e. for capture from the $2p, m=0$ initial state, the difference between the IA and the transverse peaked SPB is similar as for a $1s$ initial state. Also, the transverse peaked IA is rather close to the IA in the whole velocity range considered, such that we do not expect large changes when the peaking is dropped in the SPB calculations.

In the case of the $2s$ and $2p, m=1$ state, the peaking approximation gives much poorer results, and also the deviation of the peaked SPB from the impulse approximation is much larger, especially at the lower collision velocities. In order to study the accuracy of the transverse peaked SPB, we compare in Fig. 2

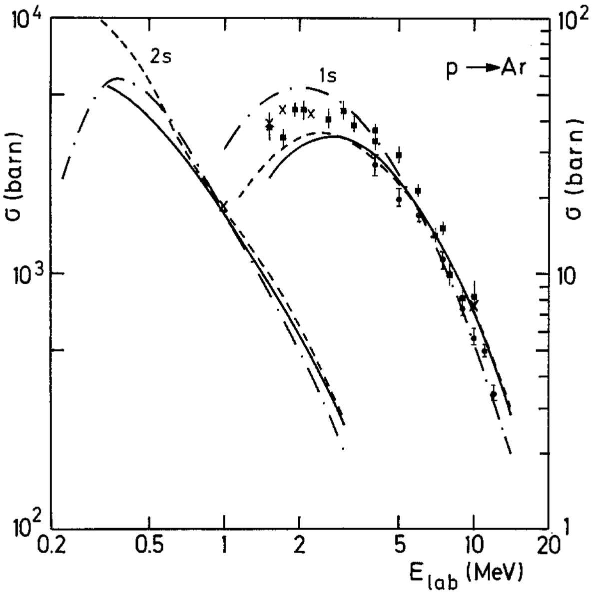

Fig. 2. Cross section for capture from the $2s$ state (left-hand scale) and from the $1s$ state (right-hand scale) of Ar by protons as a function of projectile energy. Full curves and broken curves denote SPB calculations with the renormalised and transverse peaking, respectively, and the chain curves are IA calculations. The crosses refer to an exact SPB calculation, and the experimental data are from Refs. [11] (⧫) and [12] (▪)

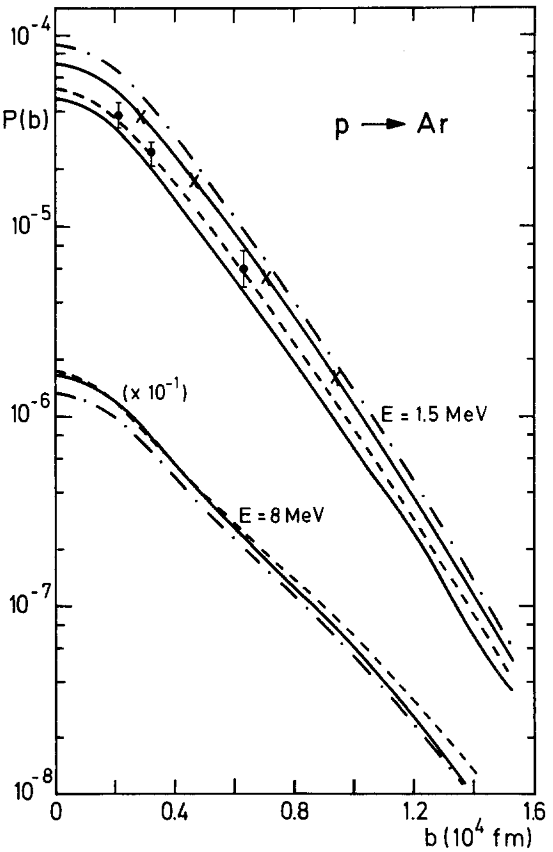

Fig. 3. Capture probability from the Ar K shell by 1.5 and 8 MeV protons as a function of impact parameter b. Full curves and broken curves denote RP and TP-SPB calculations, respectively, the chain curves are IA calculations, and the crossed curve (—×—×—) is the exact SPB. Experimental data are from [12]

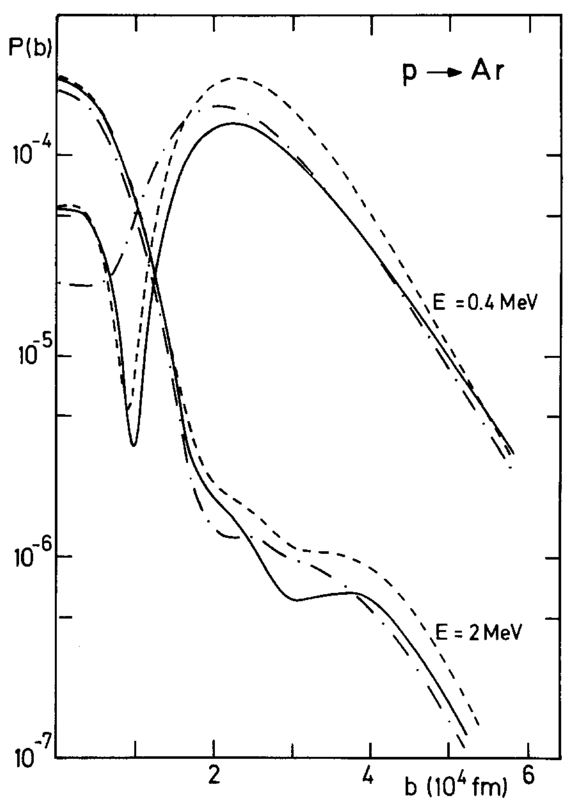

Fig. 4. Capture probability from the Ar $2s$ subshell by 0.4 and 2 MeV protons as a function of impact parameter b. The curves have the same meaning as in Fig. 3

with the less restrictive renormalised peaking. While for a $1s$ initial state, the two peaking approximations give similar results, the RP reduces the cross section by as much as a factor of 2 at low v in the case of the $2s$ state.

At low velocities, the inclusion of the off-shell effect shifts the maximum of the capture cross section to much lower velocities for all L subshells. For high velocities on the other hand, the SPB calculations give only a small increase as compared to the IA and can thus not explain the high experimental cross sections [7, 8]. We do not expect that this fact is changed in the case of unpeaked SPB calculations, because the RP and TP approximations converge at high v.

A more sensitive test of the theories is the impact parameter distribution, rather than total cross sections. Figs. 3 and 4 show the transition probability $P(b)$ as a function of b for capture from the $1s$ and $2s$ state, respectively. For transfer from the K shell, the b-dependence is rather insensitive to the theories applied, and it is mainly the absolute value of $P(b)$ which is changed. Note that at the higher projectile energy, the IA and the RP give nearly the same result, except for very small b.

For the $2s$ state, the nodal structure of the initial state wavefunction allows for a more subtle investigation of the off-shell effect, and there appears a substantial difference between the IA and the SPB results. Not only are the positions of the maxima and minima of $P(b)$ shifted, but there is also a deep minimum at the projectile energy of 0.4 MeV which is not present in the IA. On the other hand, the two SPB approximations, although showing large deviations from each other, agree roughly in the shape.

Finally we compare the SPB theory with experimental data [11, 12] in the case of capture from the K shell of Ar. As at high collision energies several investigations have shown that the SPB is the appropriate theory to explain the experiments [5, 6, 10], and because the peaked versions of the SPB give nearly identical results, we confine ourselves to the low-energy region. There, the TP and RP calculations deviate by up to 20% and are considerably lower than the measured cross sections.

An evaluation of the SPB without any peaking approximation increases the cross section due to the additional contribution of bound intermediate electron states which are neglected in the peaked versions of SPB, but which are important at low momentum transfer, i.e. around the maximum of σ. The calculated points are in good agreement with the low-velocity data (Fig. 2) thus providing evidence for the applicability of the SPB also at rather low velocities. Note that one should add about 10% to all theoretical values [14] as transfer to excited states is included in experiment, but not in theory.

In Fig. 3 the impact parameter distribution at $E = 1.5$ MeV is compared with experiment. Here, the exact SPB overestimates slightly the data. As the experimental b-dependence is well reproduced, it is not clear why the nearly identical values of the total capture cross sections do not imply a better agreement of the absolute $P(b)$.

5. Conclusion

We have calculated the capture probability from the initial K and L subshells of Ar to the ground state of hydrogen, using the transverse peaked strong potential Born theory, a less restrictive peaking (RP) in the case of initial s states, and the exact SPB for the capture from the K shell. We found that the effect of off-shell wavefunctions is smallest for the $1s$ and $2p, m=0$ initial states, while the difference as compared to the impulse approximation is rather large for the $2s$ and $2p, m=1$ initial states, especially at the lowest velocities investigated. For transfer from the L shell, SPB produces a shift of the maximum of the cross section to smaller velocities. An investigation of the impact parameter dependence shows that IA and SPB give the same slope of $P(b)$ for $1s$ and $2p, m=0$ states, while SPB decreases much stronger at small b and also at large b (for the lower velocities) in the case of the $2p, m=1$ subshell. For capture from the $2s$ state, not even the positions of the extrema of $P(b)$ are the same.

When comparing the two peaking versions of SPB, their results show also considerable deviations at small v especially for the $2s$ state, thus indicating that the peaking approximations begin to break down in this velocity region. The calculation of the capture cross section from the K shell with the exact SPB at low velocities shows good agreement with recent experimental data, which supports the conclusion that the SPB is able to explain the physics even at collision velocities which are considerably smaller than the electronic orbiting velocity v_e in its initial state. One should note, however, that the difference between SPB and IA diminishes when the peaking approximations are relaxed. It is below 30% for $1s$ transfer at $v \sim v_e/2$ which is definitively smaller than the first predictions [4]. More than experiments on total capture cross sections, detailed data on the impact parameter dependence of L-subshell capture would help to elucidate the importance of electronic off-shell states.

I would like to thank S. Alston for enlightening discussions and the GSI Darmstadt for financial support.

References

1. Briggs, J.S., Macek, J.H., Taulbjerg, K.: Com. At. Mol. Phys. **12**, 1 (1982)
2. McDowell, M.R.C., Coleman, J.P.: Introduction to the theory of ion-atom collisions. Chaps. 6–8 and p. 364. Amsterdam: North-Holland 1970
3. Briggs, J.S.: J. Phys. B**10**, 3075 (1977)
4. Macek, J., Taulbjerg, K.: Phys. Rev. Lett. **46**, 170 (1981)
5. Jakubaßa-Amundsen, D.H., Amundsen, P.A.: J. Phys. B**14**, L705 (1981)
6. Macek, J., Alston, S.: Phys. Rev. A**26**, 250 (1982)
7. Rødbro, M., Horsdal Pedersen, E., Cocke, C.L., Macdonald, J.R.: Phys. Rev. A**19**, 1936 (1979)
8. Jakubaßa-Amundsen, D.H.: J. Phys. B**14**, 2647 (1981)
9. McGuire, J.H., Sil, N.C.: Preprint (1983)
10. Alston, S.: Phys. Rev. A**27**, 2342 (1983)
11. Macdonald, J.R., Cocke, C.L., Eidson, W.W.: Phys. Rev. Lett. **32**, 648 (1974)
12. Horsdal Pedersen, E., Cocke, C.L., Rasmussen, J.L., Varghese, S.L., Waggoner, W.: J. Phys. B**16**, 1799 (1983)
13. Kelsey, E.J., Macek, J.: J. Math. Phys. **17**, 1182 (1976)
14. Jakubaßa-Amundsen, D.H., Amundsen, P.A.: Z. Phys. A – Atoms and Nuclei **297**, 203 (1980)
15. Abramowitz, M., Stegun, I.A.: Handbook of Mathematical Functions. New York: Dover Publications 1965

D.H. Jakubaßa-Amundsen
Physik-Department
Technische Universität München
Theoretische Physik
James-Franck-Strasse
D-8046 Garching bei München
Federal Republic of Germany